AN EXPERIMENTAL INVESTIGATION OF SINGLE FRACTURE FLOW BEHAVIOR UNDER NORMAL AND SHEAR LOADS

Prepared for

U.S. Nuclear Regulatory Commission
Contract No. NRC–02–07–006

Prepared by

Sitakanta Mohanty
Simon Hsiung

Center for Nuclear Waste Regulatory Analyses
San Antonio, Texas

September 2011

ABSTRACT

This report presents an experimental apparatus designed for a laboratory study of the effect of normal and shear loads on the coupled mechanical–hydrological response of a single, natural fracture (rock joint) in a relatively large-sized specimen {200 × 200 mm [8 × 8 in] fracture surface area}. Because of the practical difficulties in measuring shear load effects on permeability in natural rocks, relatively few experimental data are available in the open literature for such conditions on large specimens. The direct-shear test apparatus described in this paper is capable of measuring changes in fracture hydraulic conductivity (or permeability) using a variety of fluids injected in linear and radial flow configurations under normal and shear loads. The test apparatus enabled measurements of permeability for shear displacements of up to 2.54 cm [1 in], an improvement over previous devices. The normal stress experiments were conducted using both radial and linear flow configurations and the shear displacement experiments were conducted using only the linear flow configuration. The linear flow experiments provided a better fracture area coverage during flow than the radial flow experiments. The experiments found that an increase in normal stress to 8 MPa [1,160 psi] changed fracture permeability by nearly 35 percent, and gouge production during shearing changed fracture permeability by 300 percent at the 5-MPa [725-psi] normal stress level. The shear displacement experiment results show that gouge production can be a significant factor affecting rock joint permeability. Experiments of this kind are valuable for obtaining a better understanding of which key mechanical parameters influence fracture flow and providing data that could be used in evaluating modeling capabilities for coupled mechanical–hydrological processes.

CONTENTS

FIGURES

TABLES

ACKNOWLEDGMENTS

This paper was prepared to document work performed by the Center for Nuclear Waste Regulatory Analyses (CNWRA®) for the U.S. Nuclear Regulatory Commission (USNRC) under Contract No. NRC–02–07–006. The activities reported here were performed on behalf of the USNRC Office of Nuclear Material Safety and Safeguards, Division of High-Level Waste Repository Safety. The paper is an independent product of CNWRA and does not necessarily reflect the views or regulatory position of USNRC.

The authors gratefully acknowledge T. Wilt for his technical review, R. Lenhard for his programmatic review, L. Mulverhill for her editorial review, and L. Neill and A. Ramos for their administrative support. The authors also gratefully acknowledge the excellent comments provided by R. Fedors (NRC) and M. Nataraja (NRC).

QUALITY OF DATA, ANALYSES, AND CODE DEVELOPMENT

DATA: All CNWRA-generated original data contained in this report meet the quality assurance requirements described in the Geosciences and Engineering Division Quality Assurance Manual. Sources for other data should be consulted for determining the level of quality for those data.

ANALYSES AND CODES: No codes were used in the analyses of the work described in this report.

1 INTRODUCTION

Understanding fluid flow and transport in rock fractures (or joints) is important to many engineering and geological applications, including disposal of high-level nuclear wastes in geologic media, oil/gas exploration and production, geothermal energy exploration and production, dam stability, remediation of contaminated sites, understanding of diagenetic processes and fault sealing, and understanding the genesis of earthquakes (Nemoto, et al., 2009; O'Brien, et al., 2003). In many of these applications, the prediction of flow and transport is complicated by the coupled processes that govern flow in fractures.

In the disposal of high-level radioactive waste, flow and transport may be perturbed by thermal-mechanical–hydrological–chemical coupled processes over a long period by the radioactive waste's decay heat (Ghosh, et al., 1994). Fractures are continuously encountered in many potential host rocks for a repository for the disposal of high-level radioactive waste. The disposal tunnel excavation, dynamic ground motion from earthquake and nearby underground weapon testing, and the rock thermal expansion can change the mechanical stress state of the rock mass. These deformations can cause the joint to dilate, close, and shear, leading to changes in the joint hydrological properties, thus giving rise to mechanical-hydrological coupling.

Field evidence suggests significant mechanical–hydrological coupling effects. Geohydrological analysis in the Stripa Site Characterization and Validation Project overpredicted inflow to a drift by an order of magnitude (Ohlsson, et al., 1992). The lower measured value was attributed to potential reduced inflow due to excavation-induced stress changes. These stress changes cause the joints around the drift to open or close, which in turn strongly affects the hydraulic permeability (Rutqvist, 1995). Similarly, Loma Prieta earthquake presents an example of earthquake-induced hydrologic changes. This earthquake led to increased joint permeability resulting in the water table in the mountains dropping more than 21 m [69 ft] while greatly increasing the flow of springs and streams in the foothills (Rojstaczer and Wolf, 1992).

By definition, a mechanical-hydrological coupled process in a rock joint is a two-way process in which the mechanical stress affects fluid flow and the fluid pressure affects the mechanical condition (e.g., the effect of fluid pressure buildup on rock deformation). The majority of coupled mechanical-hydrological process studies have focused on the former. The mechanical stress effects on fluid flow have been studied both numerically and experimentally at field and laboratory scales. Predictive models for studying ensemble behavior of fractures (e.g., scaling) estimate flow and transport involving networks of fractures in porous matrices. However, fracture network flow characteristics are governed by the characteristics of flow in a single fracture. Stress-transmissivity relations reflecting behavior in a single fracture are typically provided as input to fracture network coupled process models. Therefore, research is needed to better understand the stress-transmissivity relationship for a single fracture. The most fundamental parameter is fracture permeability.

Most past studies have estimated fracture permeability as a function of normal stress (e.g., Barton, et al., 1985; Hakami and Larsson, 1996; Pyrak-Nolte, et al., 1987; Raven and Gale, 1985; Raven and Gale, 1985; Sundaram, et al., 1987; Witherspoon, et al., 1980) and very few as a function of shear stress (Bandis, et al., 1985; Makurat, 1985). Both laboratory experiments (Makurat, et al., 1990; Raven and Gale, 1985) and field testing (Carlsson and Olsson, 1986; Jung, 1989; Rutqvist, et al., 1990) have shown that the flow rate along a single joint can be highly sensitive to the change in joint aperture. Therefore, fluid flow through the

fracture network system under deformation may be affected by the deformation of this fracture network (Rutqvist, 1995). The fracture permeability studied under joint shear is somewhat limited primarily because the experiment is more difficult to conduct than similar experiments under normal stress and the experiments are even more difficult if other coupled processes are studied simultaneously. Investigators have overcome some of the experimental difficulties by using very small specimens or limiting shear displacement. Table 1-1 shows a quick-view summary of the shear displacement experiments conducted by several groups of investigators. These experiments differ in a variety of aspects including rock material (real rock and replicas), specimen shape (prismatic versus cylindrical), specimen size, fluid injection pattern for hydrological experiments (linear versus radial), shear displacement type (translational versus rotational), shear displacement extent, and applied normal load during rock shear. The variations in some cases reflected different objectives for the experiments and also reflected experimental limitations. For example, while Faoro, et al. (2009) showed large shear displacement, an artificial fracture was used for the experiment. Likewise, though Lee and Cho (2002) conducted linear flow experiments on large specimens, the shear displacement was very limited.

The objectives of the study presented in this report were to develop an experimental setup for studying coupled mechanical–hydrological process using a single rock joint and to understand fracture flow characteristics, especially permeability, under normal and shear loads. The study involved large specimens and large shear displacements. Large specimens have the advantage of large joint surface area and hence better spatial averaging for obtaining fracture permeability. The report first describes the development of the experimental technique and then the flow experiments (radial and linear) under combined normal and shear loads. This report does not make any attempt to study the scaling effects.

Table 1-1. Selected Previous Studies on Permeability Measurement Under Shear Displacement					
Investigators	**Material**	**Specimen Shape and Size, mm [in]**	**Fluid Injection Pattern**	**Normal Stress Which Shear Displacement Was Carried Out**	**Maximum Shear Displacement**
Obcheoy, et al. (2011)*	Artificial fracture made out of marble and granite	Prismatic 100 (L) × 100 (W) × 76 (H) mm [3.94 × 3.94 × 2.99 in]	Radial	3.1 MPa [450 psi]	10 mm [0.39 in]
Faoro, et al. (2009)	Artificial fracture	Prismatic 70 × 45 × 12 mm [2.76 × 1.77 × 0.47 in]	Appeared to be linear	5–20 MPa [725–2,901 psi]	15–18 mm [0.59–0.71 in]
Auradou, et al. (2006)	Transparent epoxy casts	Prismatic 12.8 × 12.8 × ? mm [0.50 × 0.50 × ? in]	Radial	0 MPa [0 psi]	A few mm
Lee and Cho (2002)	Prefractured samples of granite and marble	Prismatic 160 × 120 × 120 mm [6.30 × 4.72 × 4.72 in]	Linear	1–3 MPa [145–435 psi]	15 mm [0.59 in]
Yeo, et al. (1998)	Epoxy resin	Prismatic 200 × 200 × ? mm [7.87 × 7.87 × ? in]	Radial and Linear	0.01 MPa [1.45 psi] normal stress applied after the shear boxes reached a predetermined offset	2 mm [0.08 in]
Esaki, et al. (1995)	Prefractured samples of granite	Prismatic 120 × 100 × 80 mm [4.72 × 3.94 × 3.15 in]	Radial	20 MPa [2,901 psi]	20 mm [0.79 in]
Olsson and Brown (1993)	Natural joint of chalk	Cylindrical 60.3 (OD) × 20 (ID) mm [2.37 × 0.79 in]	Radial	4.3 MPa [624 psi]	3.5 mm [0.14 in]
Boulon, et al. (1993)	Natural and prefractured joint of granite	150 × 150 × ? mm [5.91 × 5.91 × ? in]	Linear (flowing from center to both ends) (?)	Apply normal stress after the shear displacement under 0.0 normal stress	1.82 mm [0.07 in]
Teufel (1987)	Prefractured samples of sandstone	Cylindrical 47.6 (OD); 118–124 (L) mm [1.87; 4.65–4.88 in]	Unknown	53–64 MPa [7,687–9,282 psi]	7 mm [0.28 in]
Makurat (1985)	Concrete casts	Cylindrical 150 (OD); 150 (L) mm [5.91; 5.91 in]	Linear	0.82 and 8.2 MPa [119 and 1,189 psi]	5 mm [0.20 in]

*Reference details are in the Section 6, References, of this report
Abbreviations: L–length; W–width; H–height; OD–outer diameter; ID–inner diameter;
Note: "?" indicates information was not readily available from the referenced paper.

2 EXPERIMENTAL APPARATUS

2.1 Mechanical Loading

The coupled mechanical–hydrological experimental apparatus was a direct shear test apparatus designed for testing large-sized single rock joint specimens under combined normal and direct shear loads. The test apparatus was designed, fabricated, and assembled at Southwest Research Institute® (SwRI®) (Hsiung, et al., 1994; Kana, et al., 1991). The apparatus consisted of vertical and horizontal servo-controlled loading actuators, reaction frames, shear box fixtures, and an instrumented jointed rock specimen (Figure 2-1).

The apparatus had three vertical actuators {0.133 MN [30,000 lb] in capacity} set at 120 degrees about the specimen's vertical centerline to apply normal load to the specimen. The bottom of each of the three vertical actuators was pinned to the base plate (Figure 2-1). The total normal load was controlled at a preselected value and applied to the specimen via the normal load frame that acts on the three normal load rollers. The normal load frame was designed to provide constraints to three degrees of freedom: (i) vertical translation, (ii) rotation about the horizontal axis in line with the shear, and (iii) rotation about the horizontal axis transverse to the shear.

The horizontal actuator {0.222 MN [50,000 lb] in capacity} produced direct shear to the upper specimen box, which acted through a spherical coupling. This coupling allowed for slight misalignment in the horizontal shearing motion and elevation changes of the upper specimen due to vertical load, joint surface roughness, and progressive wear. The horizontal translation of the upper specimen along the direction of shearing was guided by three rollers between the top shear box and normal load frame and side rollers. The horizontal actuator could be operated in either load or displacement control mode with loading patterns including pseudostatic and dynamic input.

A shear box housed the rock joint specimen. The bottom portion of the specimen was longer than the top portion. The shear box was designed to house top and bottom portions of a rock joint specimen separately with the maximum specimen dimension of 203 × 203 × 102 mm [8 × 8 × 4 in] for the top half and 305 × 203 × 102 mm [12 × 8 × 4 in] for the bottom half. Both top and bottom specimen parts were grouted in their respective specimen boxes by cement. The bottom shear box was bolted to a 1.22 × 2.13 × 0.15 m [4 × 7 × 0.5 ft] steel base plate for rigidity.

Vertical displacement transducers were installed to measure vertical displacements between the two rock blocks in response to the applied static normal load. These were installed at four locations (two at each side of the specimen) near the joint interface (Figure 2-1). Measurements near the interface are desirable to reduce the effects of slack or lack of strength in the grout. Proximity (noncontacting) eddy–current sensing type transducers were used to allow horizontal movement of the two joint surfaces and to measure only the vertical displacement changes continuously. The four vertical measurement points could be used to resolve the rigid body displacement of the upper block relative to the lower specimen block.

The upper and lower shear boxes were sized such that when the specimen blocks were grouted, approximately a 25.4-mm [1.0-in] gap would be left between the box faces. The side plates of each half of the specimen box were slotted, so that vertical proximeter supports and target plates could be mounted directly onto the sides of respective specimen halves. Two

(1) Vertical Load Cell No. 1
(2) Vertical Load Cell No. 2
(3) Vertical Load Cell No. 3
(4) Analog Summation of Total Vertical Normal Load
(5) Horizontal Load Cell
(6) Horizontal Displacement of Top Block Relative to Bottom Block Near Actuator – LVDT1
(7) Horizontal Displacement of Top Block Relative to Bottom Block Opposite Actuator – LVDT2
(8) Horizontal Displacement of Top Block Relative to Horizontal Load Cell – LVDT3
(9) Specimen Vertical Relative Displacement Proximeter No. 4
(10) Specimen Vertical Relative Displacement Proximeter No. 5
(11) Specimen Vertical Relative Displacement Proximeter No. 6
(12) Specimen Vertical Relative Displacement Proximeter No. 7

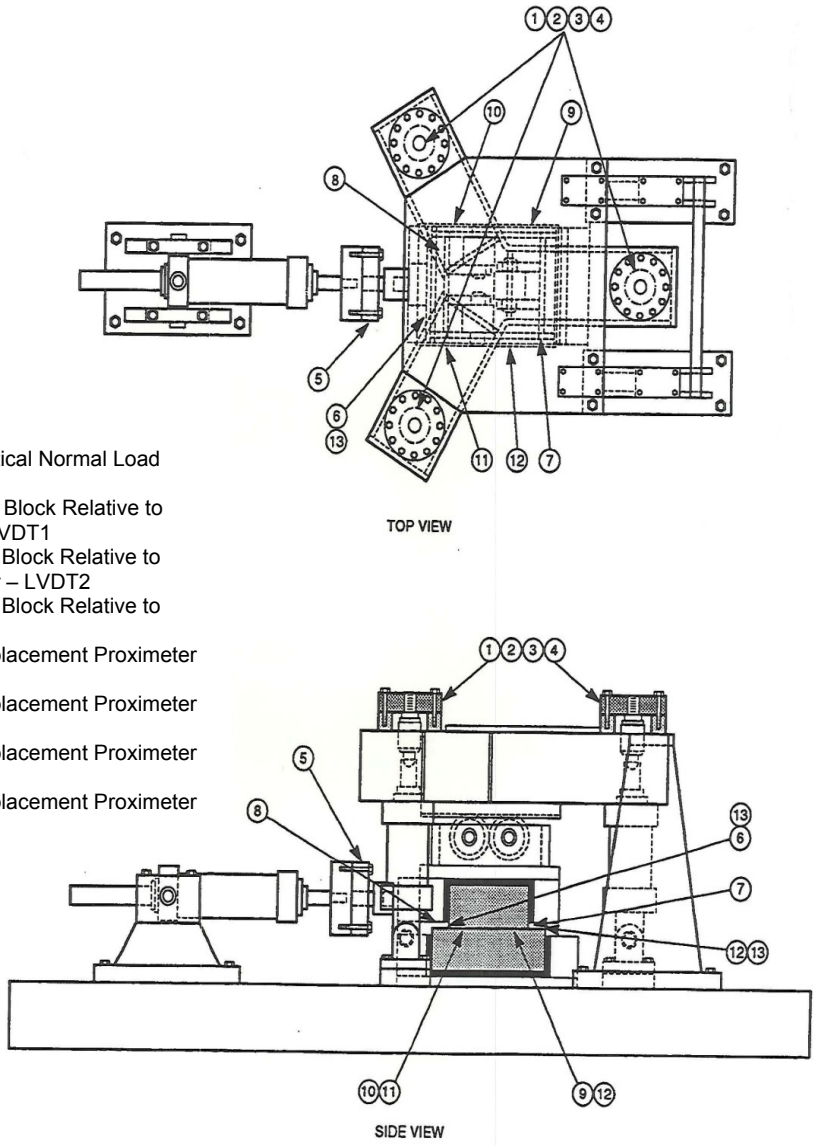

Figure 2-1. Direct Shear Test Apparatus for Flow Studies: Assembly and Instrumentation Diagram

prongs that support each plate component were cemented into lateral holes drilled into the specimen sides. The mean elevation of these 6.35-mm [0.25-in]-thick steel components was set by gauge blocks during the cementing process, so that their positions relative to the box faces were known. Although some movement of the specimen within the grout occurred during loading, the side slots were large enough so no interference occurred between the support prongs and the box side plates. Furthermore, the heavy mounting frame for the upper box side rollers was slotted so that there would be no interference between the load frame and the target plates as the upper box displaces both horizontally due to shear and vertically due to unevenness and wear of the joint interface.

Three linear variable differential transducers (LVDT), see Figure 2-1, were installed to measure the relative displacements between the top and bottom specimen blocks. Each half of a transducer was cemented directly into a hole drilled into the respective specimen block. LVDT1 was mounted on the near side of the specimen pair and LVDT2 was in the far side to provide the direct shear movement of the joint interface. LVDT3 was mounted to sense displacement of the upper block relative to the horizontal load cell. Thus, it measured any compliance that might exist in the horizontal coupling and the grout for the upper block. The position of LVDT3 was 57.2 mm [2.25 in] from the outside surface of the upper specimen box, on the same side as proximeters P4 and P5 (see Figure 2-1). A 13-channel data acquisition system coupled with an SwRI-developed software was installed to sample and record mechanical displacement data at preselected rates and times.

2.2 Fluid Flow

The apparatus was designed to carry out steady-state flow experiments after each step of normal and shear displacement. The apparatus permitted fluid flow in radial as well as linear flow configurations depending on the modifications to the specimen and the shear box. Most previous investigators used the radial flow configuration because it is a much less challenging configuration than the linear flow configuration. In this study, the radial flow configuration was used only for the normal loading condition. The linear flow configuration was used for both the normal stress and shear displacement experimental conditions. Rock specimens with the maximum top-half and bottom-half specimen dimensions allowable by the test apparatus were used for the flow experiments. The following subsections present a brief description of the theory for permeability determination and modifications to the apparatus for both flow configurations.

2.2.1 Theory

Joint permeability can be determined using Darcy's law, assuming a steady flow

$$q = \frac{kA(\Delta P)}{\mu L} \tag{2-1}$$

where ΔP is pressure drop, A is fracture cross-sectional area (m^2) [fracture aperture (b) × fracture specimen width (w)], k is permeability (m^2), q is volumetric flow rate (m^3/s) [flow velocity (v) × A], μ is dynamic viscosity of fluid (Pa–s), and L is fracture specimen length (m). For a smooth parallel plate representation of a fracture, k equals $b^2/12$. By setting up an experiment identical to the Darcy's flow experiment, the smooth parallel plate equivalent aperture can be back calculated. The single aperture by definition is representative of the

average of the aperture distribution between the two plates. For linear flow, *b* can be estimated from

$$b = \left[\frac{12 q \mu L}{w(P_1 - P_2)} \right]^{\frac{1}{3}} \tag{2-2}$$

where P_1 and P_2 are upstream and downstream pressures, respectively, and for radial flow, *b* is estimated from

$$b = \left[\frac{6 \mu q \ln \frac{r_2}{r_1}}{\pi (P_1 - P_2)} \right]^{\frac{1}{3}} \tag{2-3}$$

where r_2 and r_1 are the external and internal radii, respectively, of the fracture. For the radial flow experiments in this study, the internal radius is the inlet radius discussed in Section 2.2.2. The external radius is the radius of a circle with an area equivalent to the joint surface area of the rectangular top specimen half {203 × 203 mm [8 × 8 in]}, the smaller of the two specimen halves.

To circumvent the difficulties of a complex flow regime, it is often of interest to conduct flow experiments under a laminar flow regime with low Reynold's number. Transition from a laminar to turbulent flow regime was inferred from the Reynold's number. Turbulence may be augmented by the presence of surface roughness giving rise to eddy formation. The eddy formation due to surface roughness is usually represented by a relative roughness relation

$$R_r = \frac{\varepsilon}{D_h} \tag{2-4}$$

where D_h is the hydraulic diameter and ε is the mean height of the fracture roughness (Iwai, 1976). In this study, a gas flow experiment was also conducted. For the gas flow, the influence of gas compressibility and the Klinkenburg effect (Klinkenberg, 1941) needs to be considered. Another representation of the Reynold's number is in its reduced form for representing flow in a fracture

$$R_{e^*} = \frac{\rho v b^2}{\mu d} << 1 \tag{2-5}$$

where ρ is the fluid density and *d* is the typical distance between asperities and the average aperture must be small relative to other characteristic length scales in the problem.

2.2.2 Radial Flow Setup

For radial flow experiments, a vertical hole was drilled at the center of the upper block of the rock joint to accommodate a 6.35-mm [0.25-in] tubing. The annulus between the hole and the external wall of the tubing was sealed with epoxy. The injected fluid was allowed to exit at the

external boundary of the rock joint at atmospheric pressure. Troughs were made in the grout at the bottom and along all four sides of the bottom block and partitioned. Tubing was attached to collect and measure outflow from each face of the joint separately to permit identifying any potential preferential flow channels, which could be changing as a function of normal stress and inlet flow rate. A flow meter on the inlet line measured the constant liquid flow rate and a U-tube manometer monitored the fluid pressure changes at the injection point due to normal stress.

2.2.3 Linear Flow Setup

For linear flow experiments, the apparatus shown in Figure 2-2 was designed to inject fluid into the joint interface at one end and monitor outflow from the opposite end. Sides parallel to the overall linear flow direction were sealed to confine the flow in one direction. The grouted faces of the specimen (described later) were specially treated to prevent fluid loss. A precision positive displacement pump was used to inject liquid at a steady rate. Absolute and differential pressure transducers were used to measure the inlet and outlet fluid pressures and pressure differentials. The schematic for the flow loop for the linear flow experiment is shown in Figure 2-3.

To distribute fluid uniformly across the inlet end of the specimen, a manifold was fabricated. The manifold consisted of 1.59-mm [0.063-in] holes 5 mm [0.2 in] apart drilled in stainless steel tubing blocked at both ends. Fluid enters the manifold at its center. All these holes were aligned and pointed toward the fracture face. The tubing was split into two halves, and one half was laid against the fracture at the outlet end to ensure that the fluid would be collected from across the outlet end of the fracture. The split tube was attached to tubing to drain the fluid.

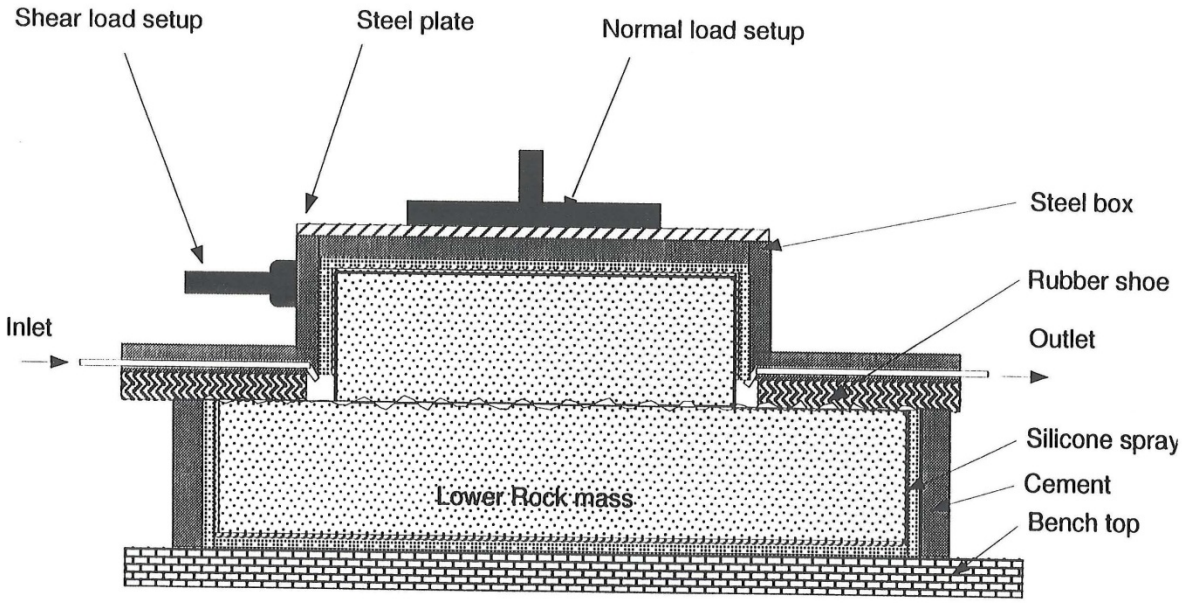

Figure 2-2. Schematic of the Linear Flow Apparatus With Normal and Shear Loading Arrangements

PT: Pressure Transducer

DPT: Differential Pressure Transducer

Core Assembly: Rock Joint Specimen Assembly

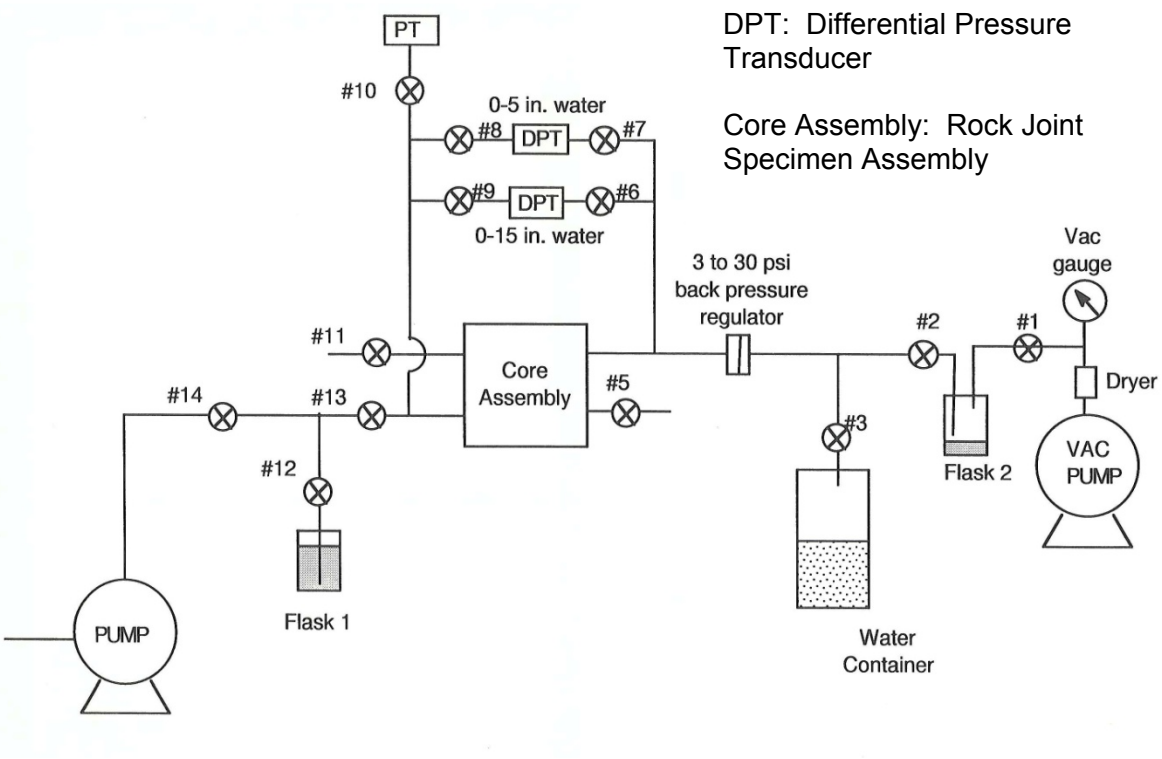

Figure 2-3. Schematic of the Flow Loop for the Linear Flow Experiment [1 in = 2.54 cm, 1 psi = 6.89 kPa]

3 EXPERIMENTAL PROCEDURE

The rock-joint specimens used in the flow tests were from a vitrified and densely welded tuff collected from Apache Leap, Arizona, (Hsiung, et al., 1994). The pores in the rock matrix hold water very tightly. The specimens used reflected the maximum dimensions allowable by the shear boxes. The surfaces were first profiled using a noncontact, surface-height-gauging profilometer (Hsiung, et al., 1994) before any instrumentation was affixed to the individual boxes.

The specimen halves were dried at 105 °C [221 °F] for 24 hours. Afterwards, they were left inside the oven for cooling with the oven door closed to minimize condensation in the pores. All surfaces of the blocks, except the joint interface, were coated with approximately 1.59-mm [0.06-in]-thick silicone rubber material and left at room temperature for 48 hours to cure. After curing, the specimen halves were grouted into corresponding boxes according to the procedure described previously in Section 2.1. The grout was left to cure for 3–4 days in the oven at 54.5 °C [130.1 °F]. Holes of different sizes were drilled onto the grouted rocks through the existing ports in the steel box. The side instrumentation supports, target plates, and LVDT mounts in both specimen halves were then installed. The gap between the hole and the instrumentation inserts was sealed with silicone rubber.

3.1 Radial Flow

Radial flow experiments were carried out as a precursor to the more elaborate linear flow experiments. Note that these experiments were carried out using rectangular blocks in shear boxes, as described in Section 2.1. The specimens were dried before starting the experiments, but fluid saturation was established by injecting fluid at high flow rates over a prolonged period. Once the system was ready, liquid flow rates were held steady at the experiments' designated rates, which ranged between 8.33 and 6,660 mm^3/s [5.1×10^{-4} and 0.41 in^3/s].

3.2 Linear Flow

For the linear flow experiments, which required sealing arrangements to confine flow in one direction (Figure 2-2), the side of the bottom specimen along the height and the contact edges were coated with silicone rubber and a gasket made of closed cell foam and fillers was emplaced on the bottom box. The gasket channels were installed on the ends of the top box, and the input and output manifolds between channels and the rock edge were mounted. The top specimen sides and the channels were coated with silicone rubber. The rubber gasket was then installed on the upper box. Both the upper and lower gasket-sealing surfaces were coated with silicone grease after the silicone rubber had set. The exteriors of the upper and lower gasket halves were coated with silicone grease, and the gasket-retaining plates were bolted onto the side of the top box.

To conduct fully water-saturated experiments, the rock specimen was evacuated *in situ* for 2 hours at 744 mm [29.29 in] Hg below atmospheric pressure with a vacuum pump (with a dehydrator to prevent water vapor from entering) and then water was allowed to be drawn into the specimen under the existing vacuum (Figure 2-3). Excess water was collected at the outlet from the flow loop in a flask that separated the vacuum pump and the specimen holder. The system was then left under a positive pressure head for several days to reach pressure equilibrium. The positive pressure was obtained by shutting the downstream-end valve off and maintaining the fluid reservoir at the inlet end 3 m [10 ft] above the specimen holder.

The fluid injected across the entire cross section using a pump was collected from the entire cross section of the opposite end. The pressure drop (ΔP) across the specimen was measured by using a differential pressure transducer. To determine air permeability, experiments were conducted using nitrogen (N_2) (because it was readily available) when the specimen was completely dry. N_2 was injected into the dry rock joint specimen at a constant rate from a high-pressure supply tank. The flow rate was controlled using a pressure regulator. The ΔP at the inlet end was measured by using a U-tube manometer, and the N_2 flow rate was measured using rotameters and digital bubble flow meters.

The downstream end was connected through a tube to a collection chamber (a large-capacity flask) placed so that there was at least 450 mm [17.7 in] of water remaining above the level of the fracture plane. This process ensured that the fracture would remain saturated even when no flow took place. This water head also ensured that air would not enter into the fracture when the mechanical loading system was deactivated and during the shearing process. At least 0.4 MPa [57.7 psi] pressure was applied to compress the rubber seal before the two rock faces came in contact with each other. The inlet tubing had sufficient water height {450-mm [17.7-in]-long tubing} to compensate for the increase in void space, keeping the joint specimen constantly saturated when changing the loading conditions.

To prevent the liquid head in the outlet tubing from falling below its entry level to the collection chamber during the shearing process (resulting in additional void due to dilation), a three-way connector was attached to the inlet end of the specimen holder. In addition, a water reservoir was connected via a valve and was maintained at such a height so that water would flow at a pressure of 3 m [10 ft].

4 RESULTS AND DISCUSSIONS

The suite of experiments involved many normal stress tests and only a limited number of shear displacement experiments with Apache Leap Tuff specimens because the shear displacement experiment is a destructive process. For normal stress experiments, both radial and linear flow configurations were used, but only a linear flow configuration was used for shear displacement experiments.

4.1 Normal Stress Experiments

To conduct flow experiments under the normal stress condition, the normal stress was increased at a preset loading rate. After the maximum normal stress {8 MPa [1,160 psi]} was reached, unloading (decreasing stress) took place at the same rate as the loading rate. At preselected load stress levels, flow was monitored.

For the radial flow configuration, the dimension of the upper block defined the outer equivalent radius in the radial flow equation because the upper block is shorter than the bottom one. Low fluid flow rates required to maintain laminar flow for Darcy's Law to apply resulted in low-pressure gradients, which were difficult to measure. Therefore, glycerol-augmented water, a higher viscosity fluid made of a mixture of water and glycerol {kinematic viscosity of 16,470 mm^2/s [16,470 cSt] at 22 °C [71.6 °F] and dynamic viscosity of 1.396×10^{-2} Pa-s [13.96 cP]} was used to increase the pressure drop at a gravitational average fluid velocity.

Table 4-1 presents the equivalent hydraulic apertures calculated at various normal stresses for the radial flow configuration, using the three fluids (air, water, and glycerol-augmented water) separately. Liquid breakthrough was observed on all but one side. The liquid breakthrough was typically one stream per side. The stream width varied slightly with the normal stress. Averaged over the entire test, 74.5, 18.4, and 7.1 percent of the total injected fluid was collected from the three sides. Despite a fourteen fold increase in the viscosity of the flowing fluid (i.e., glycerol-augmented water), the whole joint face could not be completely saturated nor was a noticeable change observed in the flow pattern. The rock specimen was saturated by flowing

Table 4-1. Equivalent Hydraulic Aperture Interpreted From Radial Flow Experiments

Normal Stress	Glycerol-Augmented		Water		Air	
	Loading	Unloading	Loading	Unloading	Loading	Unloading
0 MPa [0 psi]	0.3457 mm [0.0137 in]	0.3288 mm [0.0129 in]	0.2729 mm [0.0107 in]	0.2725 mm [0.0107 in]	—	—
1 MPa [145 psi]	0.3148 mm [0.0124 in]	0.2747 mm [0.0108 in]	0.2447 mm [0.0096 in]	0.2369 mm [0.0093 in]	0.2532 mm [0.0100 in]	0.2427 mm [0.0096 in]
3 MPa [435 psi]	0.2789 mm [0.0110 in]	0.2541 mm [0.0100 in]	0.2097 mm [0.0082 in]	0.2091 mm [0.0082 in]	0.2175 mm [0.0086 in]	0.2141 mm [0.0084 in]
5 MPa [725 psi]	0.2661 mm [0.0105 in]	0.2547 mm [0.0100 in]	0.2003 mm [0.0079 in]	0.1954 mm [0.0077 in]	0.2057 mm [0.0081 in]	0.2036 mm [0.0080 in]
7 MPa [1,015 psi]	0.2510 mm [0.0099 in]	0.2395 mm [0.0094 in]	0.1923 mm [0.0076 in]	0.1923 mm [0.0076 in]	0.1972 mm [0.0078 in]	0.1772 mm [0.0070 in]
8 MPa [1,160 psi]	0.2432 mm [0.0096 in]	0.2432 mm [0.0096 in]	0.1908 mm [0.0075 in]	0.1908 mm [0.0075 in]	0.1916 mm [0.0075 in]	0.1916 mm [0.0075 in]

water through the fracture over 2 days. The radial flow experiment provided clear evidence that most flow took place in preferential flow channels.

For the linear flow experiments, at each normal stress setting, steady-state fluid flow was established, and the ΔP across the system was recorded from differential pressure transducers at various flow rates. At each flow rate setting, steady state was allowed to be reached before ΔP was measured. A flow rate of 66.6 mm^3/s [4.1×10^{-3} in^3/s] was chosen for all normal stress tests on the basis of the Reynold's number requirement to maintain laminar flow. The experiment required precision measurements, and although fluctuations were observed in the absolute pressure measurements, our interest was in measuring the differential pressure in which there was significantly less fluctuation.

A q-ΔP plot for the linear air-flow experimental results showed a linear behavior up to a flow rate of 26.6 m^3/s [939.4 ft^3/s] corresponding to a ΔP of 4.13 kPa [0.6 psi], beyond which deviation from linearity was observed, indicating a non-Darcian flow regime.

A typical variation in mechanical and equivalent hydraulic apertures with the normal loading and unloading conditions for a joint specimen using the linear water-flow configuration is presented in Figure 4-1. The changes in hydraulic and mechanical aperture are presented as a percentage of the total span of change recorded between 0- and 8-MPa [0- and 1,160-psi] normal stress. The change in hydraulic aperture shows a hysteretic behavior similar to that observed in the change of mechanical aperture data with a slight shift at intermediate stresses. The large hysteretic behavior occurred at small normal stresses.

4.2 Shear Displacement Experiments

For shear displacement effect studies, only linear flow experiments were conducted. The shear displacement was introduced in steps. At the end of each displacement step, flow data were collected for 4 minutes. Flow data were collected with the top rock block sheared in both directions (forward and reverse). The same rock block was used for forward and reverse displacements at three different normal stress conditions. Table 4-2 shows the normal stresses for which the shear was performed and the displacement steps at which water flow data were collected. In addition, Table 4-2 presents the estimated equivalent hydraulic apertures and permeability reduction factors associated with the various normal loading and shear displacement conditions. A permeability reduction factor greater than 1.0 implies a permeability increase in response to shear displacement in a given step and a permeability reduction factor less than 1.0 imples a decrease. The data presented in Table 4-2 are from one joint specimen. The results of several joint specimens had to be discarded because of fluid leakage at high normal stress conditions.

At the end of the final displacement cycle at the 5-MPa [725-psi] normal stress, a maximum change in permeability of approximately 300 percent was observed. Because the rubber shoe at one end of the upper rock mass was suspected of blocking the outflow channel and thus raising the constricted flow effect, the upper rock was not allowed to come back to the zero position during reverse shear. The rubber shoe was later proven not to cause the constricted flow effect. During testing under 4- and 5-MPa [580- and 725-psi] normal stress, serious leaks occurred at the final displacement step of forward shearing and the initial step of the reverse shearing; hence, those data were discarded. Constricted flow effects were also observed at

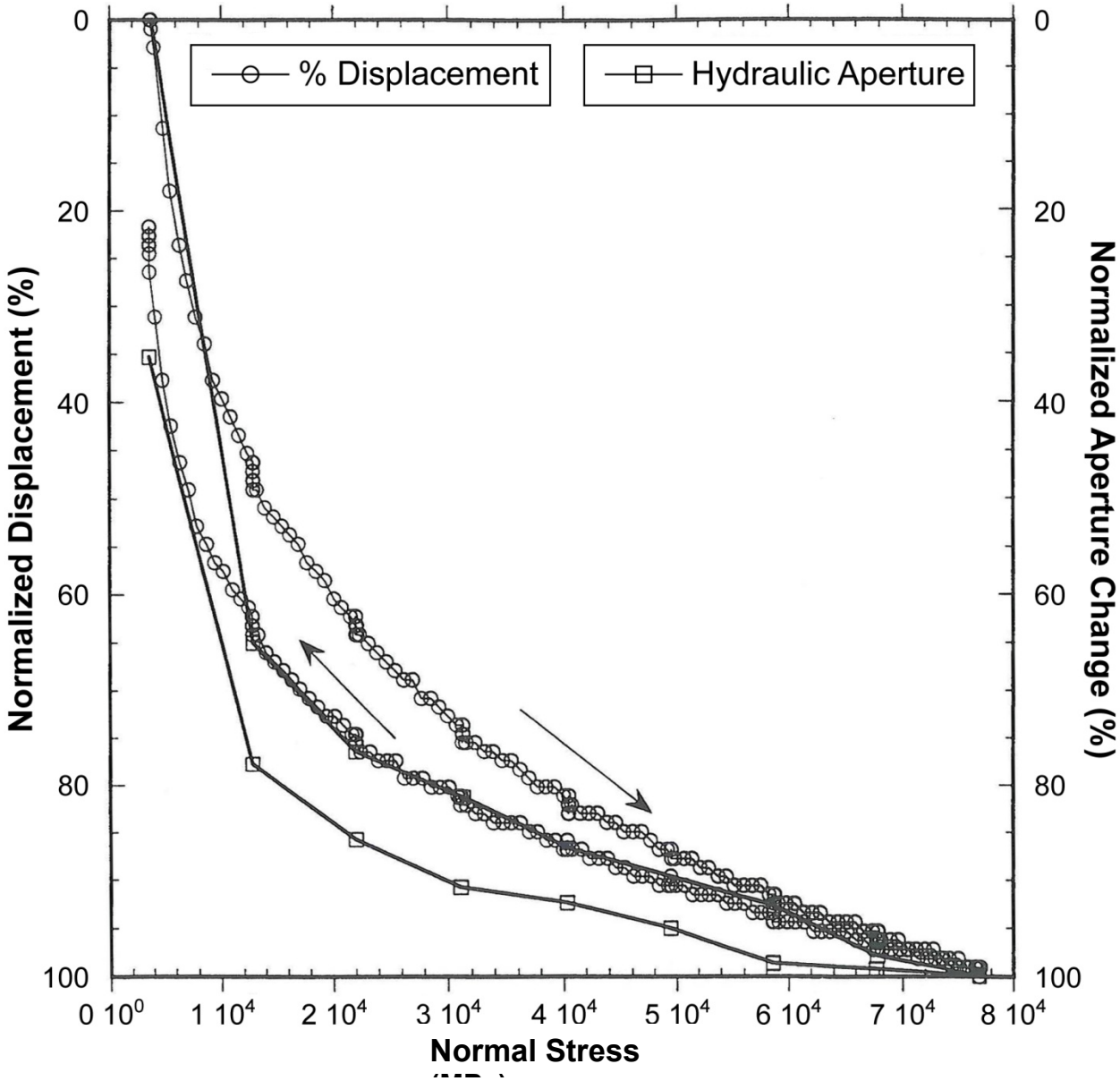

Figure 4-1. Comparison Between Relative Change in Mechanical (Displacement) and Effective Hydraulic Apertures as Normal Stress Changes. Water Was Used as the Flowing Fluid. [1 MPa = 145 psi]

several displacement steps, which were likely caused by the production and accumulation of fine particles. The migration of fine particles under a steady-state flow condition was clearly observed in the transparent tubing. Attempts were made to dislodge the blockage of flow through reverse flushing. This procedure helped clear the flow paths in only a few instances. Also, at the end of the steady-state experiment at each displacement step, particle accumulation was removed by lowering the exit end of the outlet tube, tapping the tube, and flowing water from the reservoir to dislodge the accumulated fine particles.

At the end of the experiment, the apparatus was dismantled to visually inspect the changes in the rock joint. A large amount of fine deposits in the form of a thick paste remained on the joint surface. The amount of fine deposits migrating during the flow experiment accounts for a small

portion of the fine deposits generated because of the shear. A total sum of 38.1 g [8.4×10^{-2} lb] of fine solids (including the fines in paste and the fines migrated in the flowing fluid) were dislodged from the rock specimen at the end of the final displacement cycle . Figure 4-2 illustrates the texture and size of the collected fine particles.

The maximum increase and decrease in the permeability of the fracture during 25.4-mm [1-in] shear displacement was observed to be 30 and 30 percent, respectively, with two exceptions at the 5-MPa [725-psi] normal stress (Table 4-2). It is interesting to note that, in this set of experiments, shear displacement alone does not appear to have a large effect on permeability change. The shear-displacement-induced joint dilation does result in an increase in permeability, but the joint dilation effects may be reduced by the formation of gouge materials during shearing (i.e., there are competing effects). The noticeable change in permeability that may be attributed to joint dilation could be observed between forward shearing {shear displacement of 3.61 mm [0.14 in]} and reverse shearing {shear displacement of 16.79 mm [0.66 in]} at the 4-MPa [580-psi] normal stress. During this period, the joint permeability increased 50 percent [a change in permeability reduction factor from 1.3 to 0.8 (see Table 4-2)]. Another large joint dilation effect—a 300-percent increase in permeability (a change in permeability reduction factor from 3.7 to 0.7)—could be observed at the 5-MPa [725-psi] normal stress. The large reduction in permeability (permeability reduction factor greater than 1.0) during

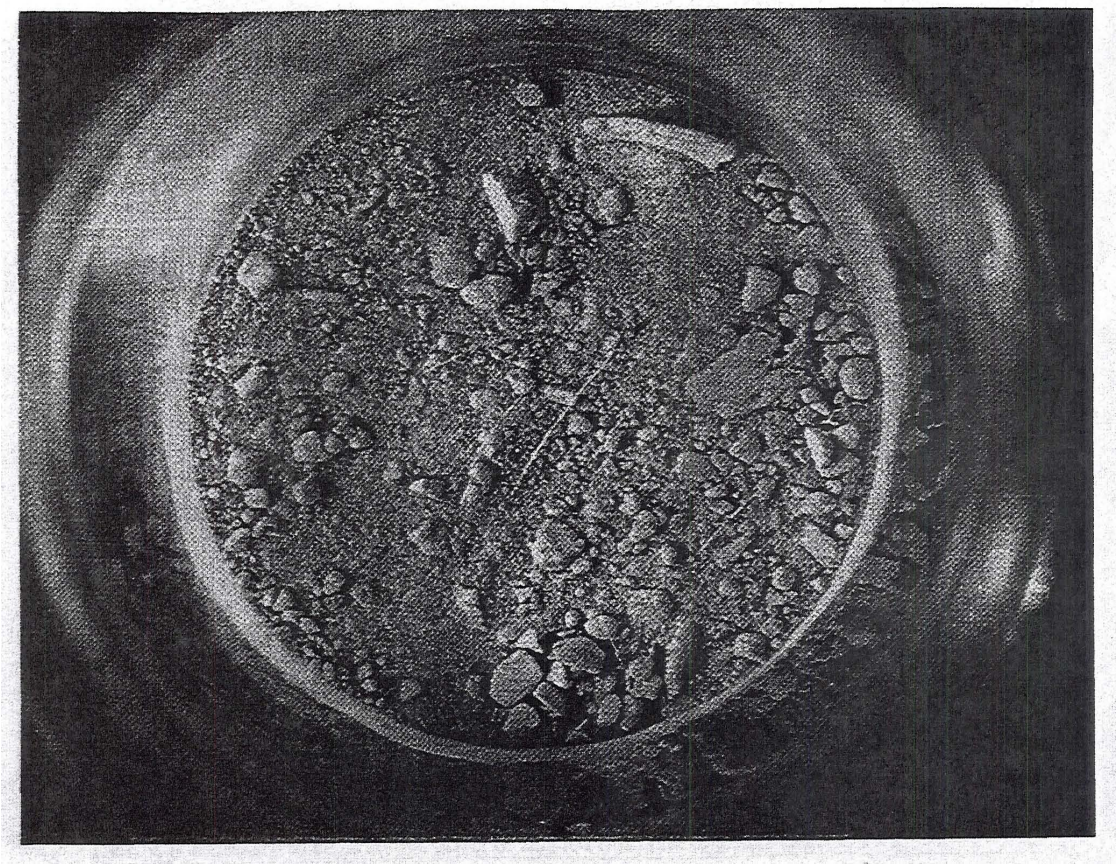

Figure 4-2. Gouge Material After Being Dried To Illustrate Texture and Particle Size

Table 4-2. Shear Displacements and Corresponding Equivalent Hydraulic Aperture During Forward and Reverse Cycles

Movement F: Forward R: Reverse	Normal Stress	Specified Shear Displacement	Hydraulic Aperture	Permeability Reduction Factor
F	2 MPa [290 psi]	4.32 mm [0.172 in]	0.12 mm [0.47 × 10^{-2} in]	1.0
		10.57 mm [0.416 in]	0.14 mm [0.55 × 10^{-2} in]	0.9
		16.66 mm [0.656 in]	0.14 mm [0.55 × 10^{-2} in]	0.9
		22.71 mm [0.894 in]	0.15 mm [0.59 × 10^{-2} in]	0.8
R	2 MPa [290 psi]	16.08 mm [0.633 in]	0.14 mm [0.55 × 10^{-2} in]	0.9
		9.80 mm [0.386 in]	0.13 mm [0.51 × 10^{-2} in]	0.9
		3.58 mm [0.141 in]	0.10 mm [0.39 × 10^{-2} in]	1.3
F	4 MPa [580 psi]	3.61 mm [0.142 in]	0.09 mm [0.35 × 10^{-2} in]	1.3
R	4 MPa [580 psi]	16.79 mm [0.661 in]	0.15 mm [0.59 × 10^{-2} in]	0.8
		10.95 mm [0.431 in]	0.13 mm [0.51 × 10^{-2} in]	0.9
F	5 MPa [725 psi]	7.11 mm [0.280 in]	0.04 mm [0.16 × 10^{-2}]	3.7
R	5 MPa [725 psi]	18.42 mm [0.725 in]	0.18 mm [0.71 × 10^{-2} in]	0.7
		17.25 mm [0.679 in]	0.15 mm [0.59 × 10^{-2} in]	0.8
		11.40 mm [0.449 in]	0.04 mm [0.16 × 10^{-2} in]	2.9

shearing observed at the 2-MPa [290-psi] and 5-MPa [725-psi] normal stresses, on the other hand, may be postulated as resulting from substantially more gouge materials being produced at these specific shearing steps than at other shearing steps, resulting in a blockage of water flow.

5 CONCLUSIONS

The change in rock-joint permeability under normal stress and shear displacement was investigated using large specimens. The apparatus demonstrated a capability for measuring the effect of up to 25.4 mm [1 in] of shear displacement on permeability, a substantial improvement over previous studies with linear flow experiment capabilities. The equipment design described in this report is such that a shear displacement of up to 50.8 cm [2 in] can be studied.

Results from testing a large rock-joint specimen showed up to a 35 percent change in fracture permeability in response to an increase in normal stress to 8 MPa [1,160 psi]. Loading and unloading the normal stress showed a definite hysteresis in the equivalent hydraulic aperture, with a similar trend being observed from the mechanical aperture (normal displacement) measurements. As expected, the equivalent hydraulic aperture showed a nonlinear trend with the imposed normal stress.

Performing shear load experiments was more difficult compared to the normal load experiments, due primarily to the extreme conditions under which the fluid-sealing mechanism functions. This difficulty is also complicated by the fact that shear testing is a destructive method of testing. Damage of the rough surface is clearly evident by the significant amount of fine particles produced. Shearing resulted in gouge material production and joint dilation. Gouge materials tend to reduce permeability, while joint dilation increases permeability. Based on the limited experimental results obtained in this study, it appears that gouge production plays a dominant role in permeability changes at high normal stress conditions. The maximum reduction in permeability (300 percent) was observed at the 5-MPa [725-psi] normal stress. However, in many instances of displacements, especially at lower normal stresses, permeability may not change significantly because of the competing effects of fracture dilation and gouge formation.

6 REFERENCES

Auradou, H., G. Drazer, A. Boschan, J. Hulin, and J. Koplik. "Flow Channeling in a Single Fracture Induced by Shear Displacement." *Geothermics*. Vol. 35. pp. 576–588. 2006.

Bandis, S.C., A. Makurat, and G. Vik. "Predicted and Measured Hydraulic Conductivity of Rock Joints." Fundamentals of Rock Joints: Proceedings of the International Symposium on Fundamentals of Rock Joints. Björkliden, Sweden: International Symposium on Fundamentals of Rock Joints. pp. 269–279. 1985.

Barton, N., S. Bandis, and K. Bakhtar. "Strength Deformation and Conductivity Coupling of Rock Joints." *International Journal of Rock Mechanics and Mining Science & Geomechanics Abstracts*. Vol. 22. pp. 121–140. 1985.

Boulon, M., A.P.S. Selvadurai, H. Benjelloun, and B. Feuga. "Influence of Rock Joint Degradation on Hydraulic Conductivity." *International Journal of Rock Mechanics and Mining Sciences and Geomechanics Abstracts*. Vol. 30. pp. 1,311–1,317. 1993.

Carlsson, A. and T. Olsson. "Large Scale *In Situ* Test on Stress and Water Flow Relationships in Fractured Rock." Technical Report. Stockholm, Sweden: Swedish State Power Board. p. 152. 1986.

Esaki, T., K. Ikusada, A. Aikawa, and T. Kimura. "Surface Roughness and Hydraulic Properties of Sheared Rock." *Fractured and Jointed Rock Masses*. L. Myer, N. Cook, R. Goodman, and C. Tsang, eds. Rotterdam, The Netherlands: Balkema. pp. 393–398. 1995.

Faoro, I., A. Niemeijer, C. Marone, and D. Elsworth. "Influence of Shear and Deviatoric Stress on the Evolution of Permeability in Fractured Rock." *Journal of Geophysical Research*. Vol. 114, B01201. DOI:10.1029/2007JB005372. pp. 1–10. 2009.

Ghosh, A., S.M. Hsiung, G.I. Ofoegbu, and A.H. Chowdhury. "Evaluation of Computer Codes for Compliance Determination Phase II." CNWRA 94-001. San Antonio, Texas: CNWRA. 1994.

Hakami, E. and E. Larsson. "Aperture Measurements and Flow Experiments on a Single Natural Fracture." *International Journal of Rock Mechanics and Mining Science and Geomechanics Abstracts.* Vol. 33, Issue 4. pp. 395–404. 1996.

Hsiung, S.M., D.D. Kana, M.P. Ahola, A.H. Chowdhury, and A. Ghosh. NUREG/CR–6178, "Laboratory Characterization of Rock Joints." Washington, DC: NRC. 1994.

Iwai, K. "Fundamental Studies of Fluid Flow Through a Single Fracture." Ph.D. Thesis. University of California at Berkeley. Berkeley, California. 1976.

Jung, R. "Hydraulic *In Situ* Investigations of an Artificial Fracture in the Falkenberg Granite." *International Journal of Rock Mechanics and Mining Science and Geomechanics Abstracts.* Vol. 26. pp. 301–308. 1989.

Kana, D.D., B.H.G. Brady, B.W. Vanzant, and P.K. Nair. NUREG/CR–5440, "Critical Assessment of Seismic and Geomechanics Literature Related to a High-Level Nuclear Waste Underground Repository." Washington, DC: NRC. June 1991.

Klinkenberg, L.J. "The Permeability of Porous Media to Liquids and Gases." *American Petroleum Institute, Drilling, and Productions Practices*. pp. 200–213. 1941.

Lee, H.S. and T.F. Cho. "Hydraulic Characteristics of Rough Fractures in Linear Flow Under Normal and Shear Load." *Rock Mechanics and Rock Engineering*. Vol. 35, No. 4. pp. 299–318. 2002.

Makurat, A. "The Effect of Sheer Displacement on the Permeability of Natural Rough Joints." Proceedings of the Hydrogeology of Rocks of Low Permeability, Tucson, Arizona. pp. 99–106. 1985.

Makurat, A., N. Barton, and N.S. Rad. "Joint Conductivity Variation Due to Normal and Shear Deformation." Proceedings of the International Symposium on Rock Joints. N. Barton and O. Stephansson, eds. Rotterdam, The Netherlands: Balkema. pp. 535–540. 1990.

Nemoto, K., N. Watanabe, N. Hirano, and N. Tsuchiya. "Direct Measurement of Contact Area and Stress Dependence of Anisotropic Flow Through Rock Fracture With Heterogeneous Aperture Distribution." *Earth and Planetary Science*. 281. pp. 81–87. 2009.

Obcheoy, J., S. Aracheeploha, and K. Fuenkajorn. "Fracture Permeability Under Normal and Shear Stresses. Proceedings of the Third Thailand Symposium on Rock Mechanics (ThaiRock 2011), Phetchaburi, Thailand, March 10–11, 2011. K. Fuenkajorn and N. Phien-Wej, eds. Nakhon Ratchasima, Thailand: Suranaree University of Technology, Institute of Engineering. pp. 133–140. 2011.

O'Brien, G.S., C.J. Bean, and F. McDermott. "Numerical Investigations of Passive and Reactive Flow Through Generic Single Fractures With Heterogeneous Permeability." *Earth and Planetary Science*. Vol. 213. pp. 271–284. 2003.

Olsson, W.A. and S.R. Brown. "Hydromechanical Response of a Fracture Undergoing Compression and Shear." *International Journal of Rock Mechanics and Mining Science and Geomechanics Abstracts*. Vol. 30. pp. 845–851. 1993.

Ohlsson, O., J. Black, J. Gale, N. Barton, L. Birgersson, C. Cosma, B. Dershowitz, T. Doe, A. Hernbert, D. Holmes, M. Laaksoharju, J. Long, and I. Neretnieks. "Site Characterization and Validation—Final Report." Stripa Project TR 92-22. Stockholm, Sweden: SKB. 1992.

Pyrak-Nolte, L., L.J. Myer, N.G.W. Cook, and P.A. Witherspoon. "Hydraulic and Mechanical Properties of Natural Fractures in Low Permeability Rock." Proceedings of the 6th International Society for Rock Mechanics Congress, Montreal, Canada. pp. 225–231. 1987.

Raven, K.G. and J.E. Gale. "Water Flow in a Natural Rock Fracture as a Function of Stress and Sample Size." *International Journal of Rock Mechanics and Mining Science and Geomechanics Abstracts*. Vol. 22. pp. 251–261. 1985.

Rojstaczer, S. and S. Wolf. "Permeability Changes Associated With Large Earthquakes: An Example From Loma Prieta, California." *Geology*. Vol. 20. pp. 211–214. 1992.

Rutqvist, J. "Determination of Hydraulic Normal Stiffness of Fractures in Hard Rock from Well Testing (Technical Note)." *International Journal of Rock Mechanics and Mining Science and Geomechanics Abstracts*. Vol. 32, No. 5. pp. 513–523. 1995.

Rutqvist, J., C.L. Ljunggren, O. Stephansson, J. Noorishad, and C.-F. Tsang. "Theoretical and Field Investigations of Fracture Hydromechanical Response Under Fluid Injection." N. Barton and O. Stephansson, eds. Rock Joints. Proceedings of the International Symposium on Rock Joints. Rotterdam, The Netherlands: Balkema. pp. 557–564. 1990.

Sundaram, P.N., D.J. Watkins, and W.E. Ralph. "Laboratory Investigations of Coupled Stress-Deformation—Hydraulic Flow in a Natural Rock Fracture." Rock Mechanics: Proceedings of the 28th U.S. Symposium, Tucson, Arizona. pp. 585–592. 1987.

Teufel, L.W. "Permeability Changes During Shear Deformation of Fractured Rock." Rock Mechanics: Proceedings of the 28th U.S. Symposium, Tucson, Arizona. Vol. 129. pp. 473–480. 1987.

Witherspoon, P.A., J.S.Y. Wang, K. Iwai, and J.E. Gale. "Validity of Cubic Law for Fluid Flow in a Deformable Rock Fracture." *Water Resources Research*. Vol. 16. pp. 1,016–1,024. 1980.

Yeo, I.W., M.H. De Freitas, and R.W. Zimmermann. "Effect of Shear Displacement on the Aperture and Permeability of a Rock Fracture." *International Journal of Rock Mechanics and Mining Science and Geomechanics Abstracts*. Vol. 35. pp. 1,051–1,070. 1998.